Carbohydrate Research 343 (2008) 2229–2234

Contents lists available at ScienceDirect

Carbohydrate Research

journal homepage: www.elsevier.com/locate/carres

Detergency effects of nanofibrillar amyloid formation on glycation of human serum albumin

Naghmeh Sattarahmady [a], Ali A. Moosavi-Movahedi [a,*], Mehran Habibi-Rezaei [b], Shahin Ahmadian [a], Ali A. Saboury [a], Hossein Heli [a], Nader Sheibani [c]

[a] Institute of Biochemistry and Biophysics, University of Tehran, Tehran, Iran
[b] School of Biology, College of Science, University of Tehran, Tehran, Iran
[c] Department of Ophthalmology and Visual Sciences, University of Wisconsin, Madison, WI, USA

ARTICLE INFO

Article history:
Received 20 October 2007
Received in revised form 26 April 2008
Accepted 29 April 2008
Available online 7 May 2008

Keywords:
Amyloid
Human serum albumin
Glycation
Surface tension
Transmission electron microscopy

ABSTRACT

The prolonged glycation of human serum albumin (HSA) results in significant changes in its structure. The identity of these structural changes and the influence of carbohydrates on these changes require further study. Here, we evaluated structural changes and amyloid formation of HSA upon incubation with Glc, Fru, or Rib. Fluorescence spectrophotometry, surface tension analysis, and transmission electron microscopy (TEM) were utilized to evaluate the structures of glycated HSA. The physicochemical properties including excess free energy, protein adsorption at the air–water interface, critical aggregation concentration (CAC), and surface activity indicated an increase in hydrophobicity and partial unfolding of HSA structure upon glycation. Thus, it appears that AGE products can act as detergents. Incubation of HSA with these sugars after 20 wks induced significant amyloid nanofibril formation. Together these results indicate that prolonged glycation of HSA is associated with a transition from helical structure to β-sheet (amyloid formation).

1. Introduction

Glycation is a common spontaneous modification of proteins in which reducing carbohydrates bind covalently to the free amino groups and undergo modifications to form a class of heterogeneous compounds collectively referred to as advanced glycated end products (AGEs).[1] The presence of AGEs has been associated with aging in several species and with the severity of some human pathologies including diabetes and Alzheimer's disease.[2,3] Glycated proteins are also used in formulated foods as functional ingredients with radical scavenging activity to prevent deterioration due to oxidation.[4]

Glycation of proteins has significant impact on their physical and functional properties. These changes in protein properties could be related to alteration in the conformation of the protein.[5] Targets of advanced glycation include structural proteins, such as collagen, plasma proteins, including albumin, and intracellular proteins such as hemoglobin.[6] Glycation of human serum albumin (HSA) is of special interest. HSA has approximately 58 Lys residues making it a favorable target for glycation.[7] HSA is quantitatively the most important depot and transport protein in blood plasma. It is a major antioxidant with important roles in maintaining normal osmolarity of plasma and interstitial fluids.[8] Therefore, the identification of the sites of glycation, structural and functional changes during glycation of HSA, and AGE formation in the presence of different carbohydrates have been the subject of many recent in vitro studies.[9–15]

The in vitro glycation rate is a function of the anomerization of the carbohydrate. The larger percentage of the open-chain form in a given carbohydrate leads to a more reactive carbohydrate.[16] The carbonyl groups of aldehydes are more electrophilic than those of ketone groups. Rib sugars and sugar phosphates undergo traditional Maillard reactions leading to a diverse set of products.[17] Rib solution has a greater fraction of the highly reactive open-chain form and can react much faster than Glc and Fru with bovine serum albumin (BSA) in glycation processes.[18] We have recently reported studies on the extent of Glc-mediated HSA glycation and its structural changes.[19–21] Here, we compared the ability of Glc, Fru, and Rib in glycation of HSA and generation of amyloid structures. We demonstrate that the prolonged glycation of HSA has a detergent-like effect on HSA structure and leads to amyloid formation in a carbohydrate-dependent manner.

2. Results and discussion

The AGE formation was detected using the quantification of the reacted Lys and Arg side-chains. Figure 1A shows the percentage of

* Corresponding author. Tel.: +98 21 66403957; fax: +98 21 66404680.
E-mail address: moosavi@ibb.ut.ac.ir (A. A. Moosavi-Movahedi).

0008-6215/$ - see front matter © 2008 Elsevier Ltd. All rights reserved.
doi:10.1016/j.carres.2008.04.036

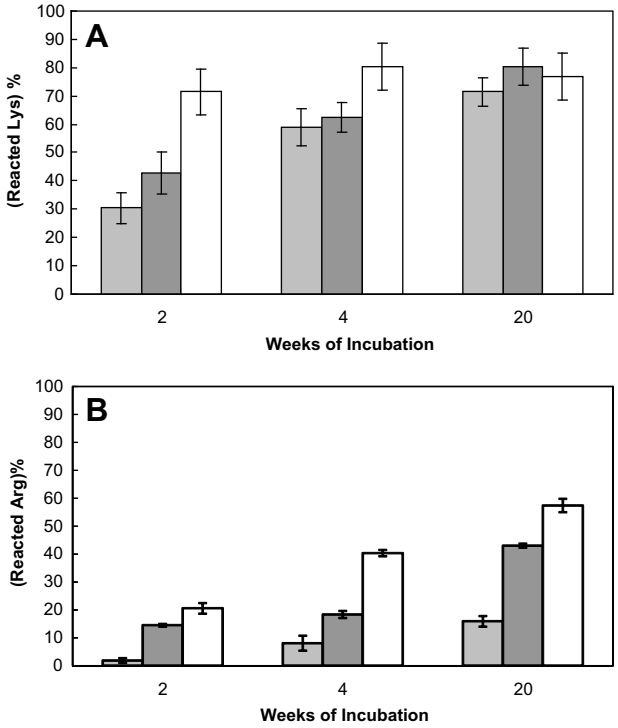

Figure 1. Percentage of reacted Lys (A) and Arg (B) residues are shown for samples of glycated HSA incubated with 500 mM Glc (▒), Fru (■), or Rib (□) for different times.

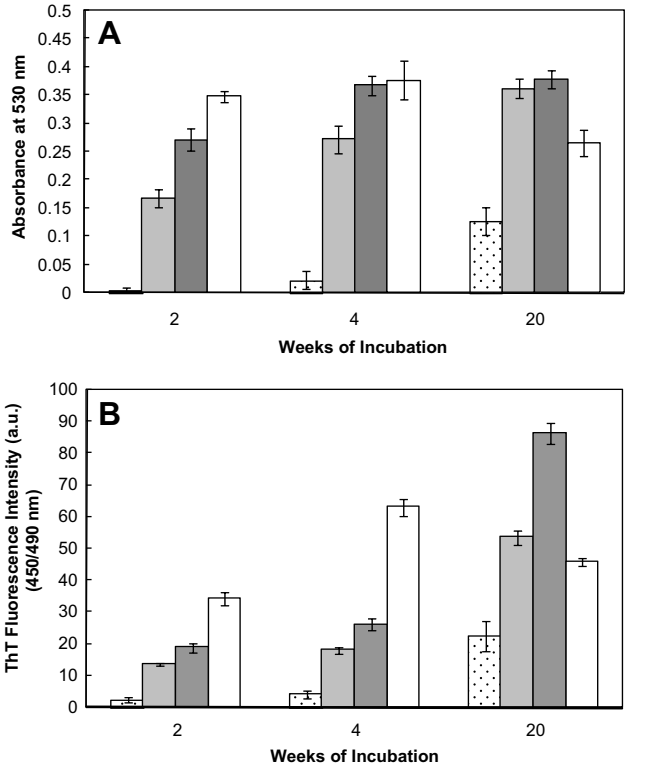

Figure 2. The columns show the absorbance of Congo red at 530 nm (A) and ThT fluorescence intensity ratios of excitation/emission at 450/490 nm (B) for samples of HSA after 2, 4, and 20 wks of incubation without any carbohydrate (▒) or with 500 mM Glc (▒), Fru (■), or Rib(□).

reacted Lys residues per mg HSA in each sample after 2, 4, and 20 wks of incubation in the presence of Glc, Fru, or Rib compared to fresh-native HSA. In fresh-native HSA all of the 58 Lys residues are free (reacted Lys is 0%). However, with increasing incubation times the percentage of reacted Lys residues gradually increased for HSA samples incubated with Glc or Fru. The maximum modification of Lys residues for HSA samples incubated with Rib was observed after 2 wks of incubation. The maximum modification of Lys residues for HSA samples incubated with Glc or Fru (~80%) was observed after 20 wks of incubation. Figure 1B shows the percentage of reacted Arg per mg HSA in each sample after 2, 4, and 20 wks of incubation in the presence of Glc, Fru, or Rib. The percentage of reacted Arg residues in glycated HSA increased gradually. The maximum modification of Arg residues in HSA samples incubated with Rib reached 57%.

Figure 2 shows the absorbance at 530 nm for the Congo red-incubated samples and fluorescence intensity for the thioflavin T (ThT), as indicators of amyloid fibril formation.[3,22] Increases in the Congo red absorbance at 530 nm, and the ThT fluorescence intensity after 2 and 4 wks of incubation, indicated formation of amyloid fibrils. Furthermore, while the ThT fluorescence intensity of the samples after 20 wks of incubation with Glc or Fru (whole solution) increased, that of samples incubated with Rib (just supernatant) decreased, confirming the presence of amorphous aggregates in the Rib supernatant (Fig. 2B). In addition, the binding of ThT to aggregates was visualized in parallel by fluorescence microscopy (data not shown). The areas rich in protein fibrous material were stained with ThT giving a bright green-yellow fluorescence against a non-bright background. No fluorescence was detected for the protein in its native state. In this way, the presence of amyloid in the glycated samples was confirmed.

To better observe the appearances of amyloid structures and forms of aggregates, the AGE-HSA samples were analyzed by TEM. Images of the sample after incubation with Glc after 20 wks of incubation (Fig. 3A–C) revealed three significantly different structural organization: uniformly distributed fine amorphous aggregates and large branched chains of globular aggregates with 20–30 nm average diameter (Fig. 3A), bundles of unbranched fibrillar aggregates with 140 nm average lengths (Fig. 3B), and large branched chains of globular aggregates with 20–40 nm average diameter (Fig. 3C). HSA control solution incubated for 20 wks in the absence of any sugar appeared as a uniformly distributed, fine amorphous precipitate, and long fibrillar states (Fig. 3D). In the TEM images of precipitates of Rib sample (Fig. 4A–C), three different structures were observed: large branched chains of globular aggregates with 25–30 nm average diameter (Fig. 4A), fibrous sheet-like structures (140 nm) that collect in the cylindrical structure (Fig. 4B), and the long straight amyloid fibrils with 15–20 nm average diameter (Fig. 4C). The supernatant of samples that were incubated with Rib after 20 wks (Fig. 4D) revealed only branched chains of globular aggregates with 30 nm average diameter. TEM images of prolonged glycation of BSA using different sugars confirmed the presence of branched chains of globular aggregates and bundles of unbranched fibrillar aggregates in solution.[3] According to the TEM images, it is thought that in the pathway of fibril formation, after formation of branched chains of globular aggregates and unbranched fibrillar aggregates, precipitates are formed. There are also other intermediates in amyloid formation before completion of the reaction.

To elucidate the mechanisms underlying glycation-induced amyloid formation, the surface activities of glycated HSA were analyzed. The stabilization of proteins in sugar medium is related to the effect of sugar molecules (co-solvent) on the surface tension of the solvent. Although, the increase in surface tension by co-solvent does not ensure increased stabilization, the binding of ligands can reduce its effects.[23] In the glycation process, the interactions of carbohydrates with the proteins affect the surface rheology of globular proteins adsorbed at an air–water interface. This behavior

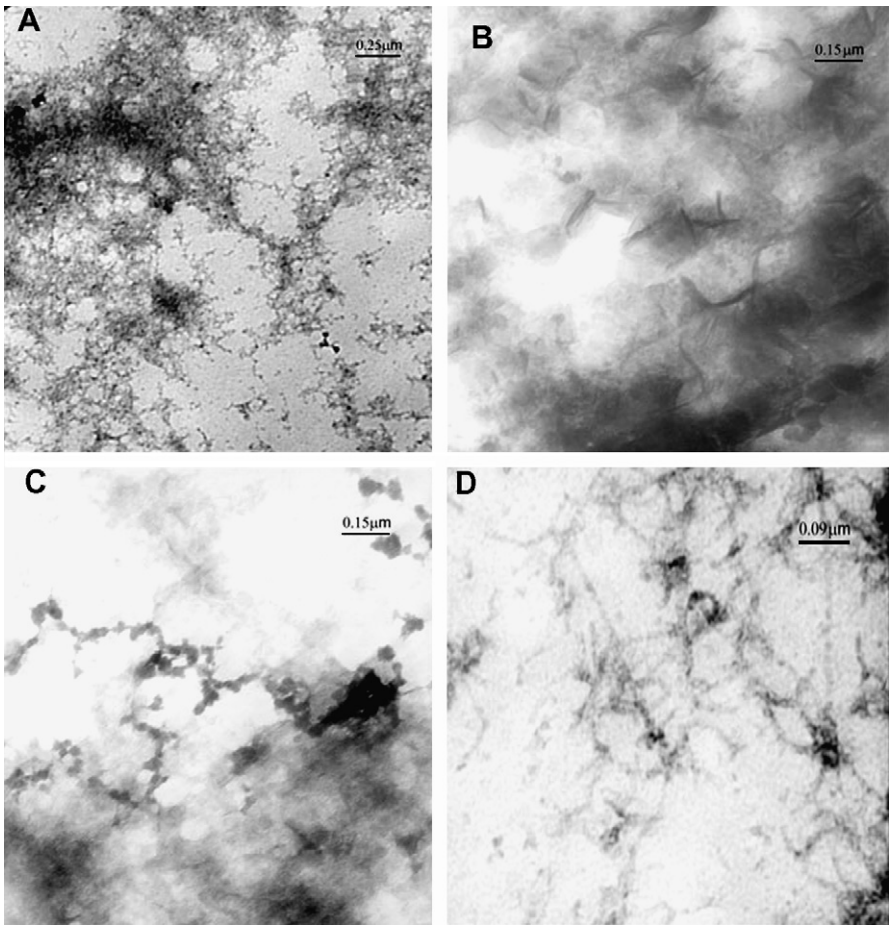

Figure 3. TEM images indicate samples of AGE–HSA incubated with 500 mM Glc (A–C) or control HSA (D) for 20 wks.

is similar to the effects of detergents on proteins in aqueous solutions, which decreases the surface tension of the protein solution.

Figure 5A shows measurements of surface tension of fresh-native and control solutions of HSA after 2, 4, and 20 wks of incubation without any carbohydrate, as a function of protein concentration. The increasing protein concentration in Figure 5A is accompanied by with a break point in the surface tension curve. This point is often termed CAC and corresponds to the concentration where the micellar aggregates become detectable. This is very similar to CMC point in detergent solutions.[24] This behavior in surface tension change of HSA agreed with those previously reported by others.[24,25] The changes in surface tension of control HSA samples after 2 and 4 wks of incubation in the absence of any carbohydrate were similar to fresh-native HSA, and showed a CAC of approximately 0.88–0.99 μM. However, after 20 wks of incubation the CAC value decreased to 0.6 μM (Fig. 5A).

The values of surface tension for glycated HSA (1 mg/mL) incubated with different sugars were measured at 25 °C (Table 1). The surface tension of 1 mg/mL native HSA was approximately 47 mN/m, but in the case of control solution after 20 wks of incubation, it was approximately 40 mN/m. The surface tension of glycated HSA decreased with longer incubation time in a sugar dependent manner. Figure 5B–D shows the variation of surface tension versus concentrations of glycated HSA incubated with different sugars for different times at 37 °C. Glc, Fru, or Rib had similar effects on the extent of CAC after 2 wks of incubation (Fig. 5B–D). However, Rib decreased the extent of CAC after 4 wks of incubation compared to Fru and Glc. Surface tension of glycated HSA in the presence of Fru or Rib decreased significantly after 20 wks of incubation.

The HSA molecules in their native (folded) state are water soluble due to the presence of hydrophilic groups at the protein surface. A strong adsorption to the interface arises from the presence of surface hydrophobic groups due to the interactions of some ligands, especially surfactants, resulting in protein conformational changes. Similar behavior occurred when HSA was glycated. Figure 5B–D shows the variation of surface tension versus concentrations of glycated HSA with different carbohydrates after different times of incubation at 37 °C. These differences in the surface tension curves could be interpreted as changes in geometrical dimension and molar areas of the protein in the unfolded state and their hydrophobicity.[26,27] The CAC point was shifted to the left (lower concentrations) for longer incubation times and the effectiveness of the sugar (Table 1 and Fig. 5).

According to Gibbs equations 1 and 2, the excess free energy (ΔG) of glycated samples can be deduced and also the extent of protein adsorption or protein excess at the interface (Γ) can be calculated from Eq. 3[28]: CAC_G (CAC of glycated HSA), CAC_N (CAC of fresh-native HSA), CAC_C (CAC of control HSA incubated for different times), and $d\gamma/d\ln c$ (the slope of the surface tension curve; γ is surface tension, and c is the protein concentration).

$$\Delta G_{C-G} = -RT \ln \frac{CAC_G}{CAC_C}, \quad (1)$$

$$\Delta G_{N-G} = -RT \ln \frac{CAC_G}{CAC_N}, \quad (2)$$

$$\Gamma = -\frac{1}{RT} \frac{d\gamma}{d\ln c}. \quad (3)$$

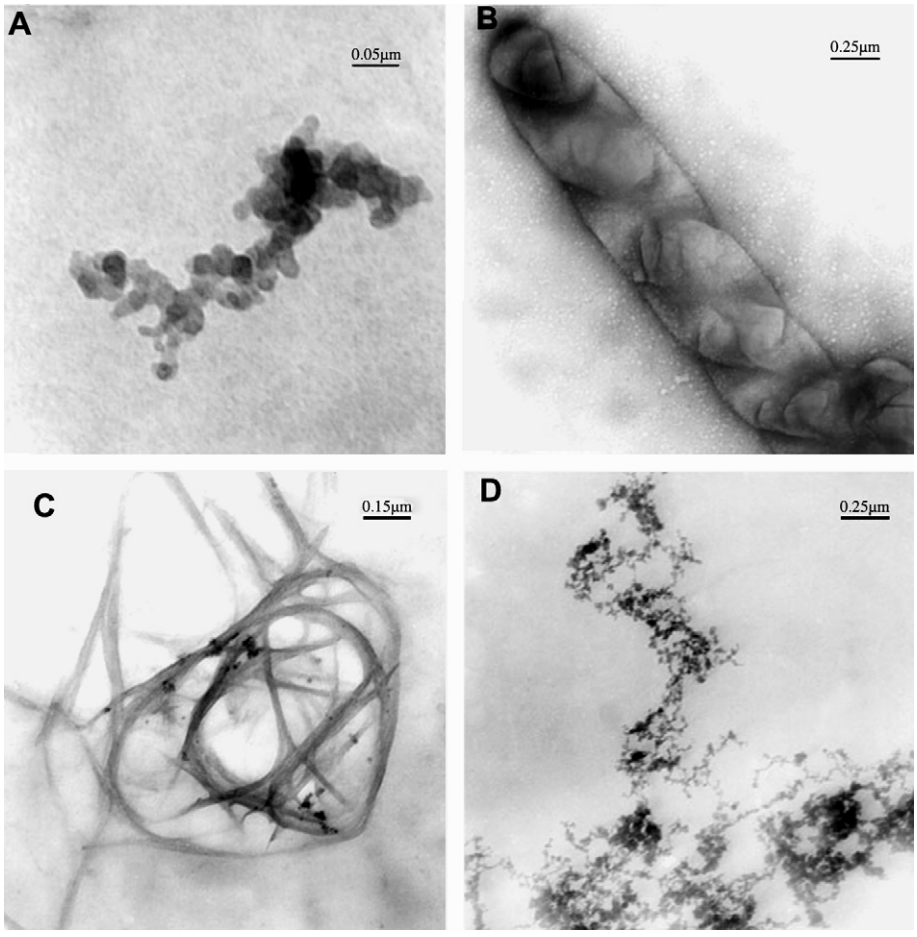

Figure 4. TEM images indicate the precipitated parts (A–C) and supernatant part (D) of samples of AGE–HSA incubated with 500 mM Rib for 20 wks.

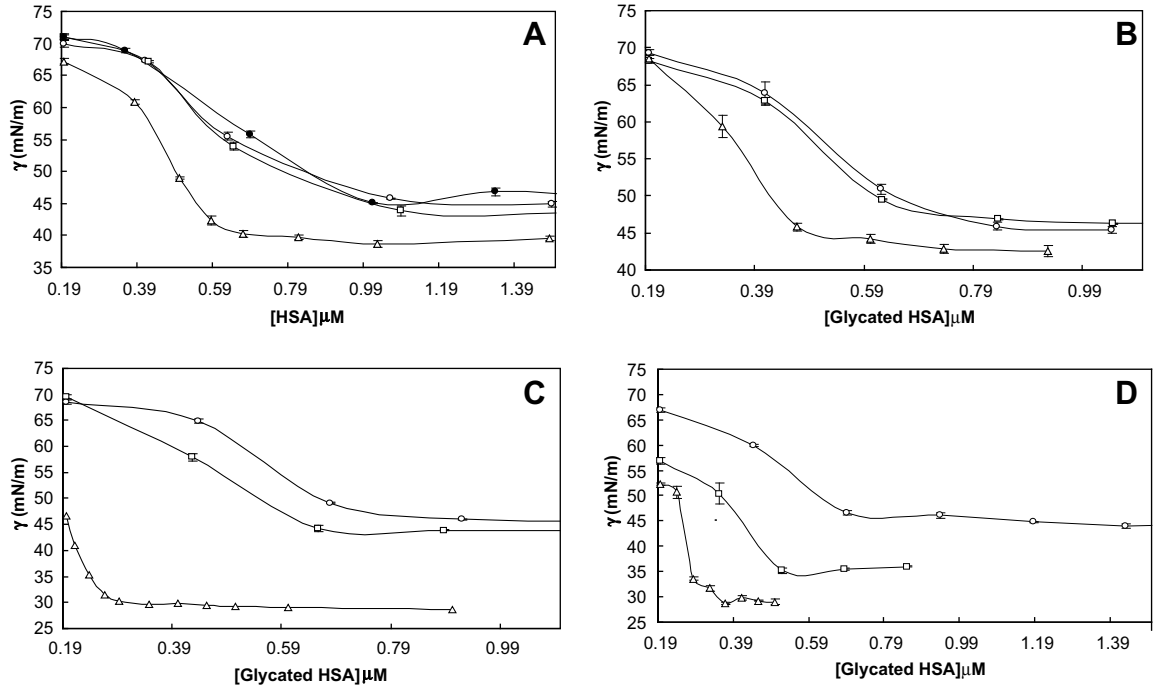

Figure 5. The curves show the surface tensions of fresh-native HSA (A; ●) and control HSA as a function of HSA concentration after 2 (○), 4 (□), and 20 (△) wks of incubation without any carbohydrate. Panels B, C, and D indicate glycated HSA incubated with 500 mM of Glc, Fru, or Rib for 2 (○), 4 (□), and 20 (△) wks, respectively.

Table 1
Surface activity characteristics of glycated HSA in the presence of different carbohydrates for different times of incubation

Weeks of incubation	Glycated HSA in the presence of glucose			Glycated HSA in the presence of fructose			Glycated HSA in the presence of ribose		
	2	4	20	2	4	20	2	4	20
$\Delta\gamma_{(N-G)}$ at 1 mg/mL protein	0.91 ± 0.34	2.59 ± 0.59	5.16 ± 0.78	1.09 ± 0.63	2.67 ± 0.59	17.79 ± 0.30	2.48 ± 0.59	13.55 ± 0.27	19.76 ± 0.70
CAC (μM)	0.70 ± 0.028	0.65 ± 0.021	0.44 ± 0.021	0.7 ± 0.002	0.67 ± 0.017	0.29 ± 0.016	0.67 ± 0.021	0.52 ± 0.03	0.27 ± 0.004
ΔG_{N-G} (kJ/mol)	0.85 ± 0.07	1.01 ± 0.06	1.98 ± 0.08	0.86 ± 0.00	0.97 ± 0.04	3.04 ± 0.09	0.97 ± 0.05	1.59 ± 0.09	3.21 ± 0.03
ΔG_{C-G} (kJ/mol)	0.62 ± 0.10	0.70 ± 0.09	0.74 ± 0.11	0.62 ± 0. 04	0.65 ± 0.08	1.80 ± 0.12	0.73 ± 0.09	1.27 ± 0.13	1.97 ± 0.05
Γ (mol/m^2)	0.0141 ± 0.0005	0.0147 ± 0.0006	0.0170 ± 0.001	0.0144 ± 0.0	0.0152 ± 0.0004	0.020 ± 0.0006	0.0155 ± 0.0002	0.0186 ± 0.0004	0.0776 ± 0.0394

Table 1 shows $\Delta\gamma_{(N-G)}$ ($\gamma_{(\text{fresh native HSA})}-\gamma_{(\text{glycated protein})}$) at 1 mg/mL protein, CAC (μM), ΔG_{N-G} (kJ/mol), ΔG_{C-G} (kJ/mol) and Γ (mol/m^2) of glycated HSA with cited sugars after different times of incubation at 37 °C. ΔG_{N-G} and ΔG_{C-G} are the excess free energy (ΔG) of glycated samples compared to fresh-native HSA and control HSA incubated for the same times in the absence of any carbohydrate. Therefore, the differences between these ΔGs represent the effects of prolonged incubation on the extent of free energy. The impact of incubation times on excess free energy in control and glycated samples incubated 2, 4, and 20 wks were approximately 0.23, 0.29, and 0.32 kJ/mol, respectively. The impact of different carbohydrates on excess free energy in glycated HSA was similar after 2 wks of incubation. However, Rib had higher impact after 4 and 20 wks of incubation. The slopes of surface tension curves in the premicellar region also indicated that the protein excess or protein adsorption at the interface was comparable with previous reports and correlated with conformational changes in the molecule.

Collectively the results of surface activity showed that glycated HSA forms micelle-like aggregates upon prolonged glycation. Glycation of HSA resulted in physicochemical changes including alterations in protein conformation. These changes are similar to interactions between proteins and surfactants in the direction of partial unfolding of the structure[29] and in the direction of transition from a helical to a β-sheet structure and nanofibrillar amyloid formation. Thus, some AGE products can act as detergents inducing amyloid nanofibril structures and decreasing CAC.

3. Experimental

3.1. Materials

HSA (⩾96%, free fatty acid), β-D (+) Glc, methylcellulose grade 20, and sodium bicinchoninate (BCA) were purchased from Sigma. The Fru, Rib, 9,10-phenanthrenequinone, and sodium azide were from Merck (Germany). ThT, Congo red, and 2,4,6-trinitrobenzene sulfonic acid (TNBSA) were acquired from Fluka. Uranyl acetate was from PELCO. All other materials were of analytical grade. All solutions were prepared with deionized water.

3.2. Procedures

For in vitro formation of AGE-HSA, HSA (10 mg/mL) was incubated with Glc, Fru, or Rib (500 mM) in 100 mM sodium phosphate buffer with 0.1 mM sodium azide in capped vials under sterile conditions at 37 °C in the dark. After 2, 4, or 20 wks of incubation, a series of vials were removed and dialyzed against sodium phosphate buffer at 4 °C for 48 h. HSA without any carbohydrate was incubated and similarly dialyzed for use as control. Following dialysis, the concentration of protein samples was determined by BCA assay. Most samples were clear and brownish yellow after incubation. However, in the samples containing Rib two phases were observed after 20 wks of incubation, a precipitate with brown stained aggregates and a supernatant that was clear and brownish yellow. The supernatant and precipitates of Rib samples were used separately for further analysis.

The determination of the level of free Lys residues was carried out using TNBSA.[10] Briefly, 4% $NaHCO_3$ and 0.1% (W/V) TNBSA were added to the protein solution, allowed to react at 37 °C for 1 h, solubilized with 10% SDS, and followed by the addition of 1 M HCl. The absorbance was then measured at 335 nm on a Shimadzu spectrophotometer model UV-3100. The number of free Arg residues in the protein was determined using 9,10-phenanthrenequinone reagent.[2] Briefly, samples of proteins were mixed with 300 μL of 9,10-phenanthrenequinone reagent (150 μM in

ethanol) and 50 μL of 2 M NaOH and incubated at 60 °C for 3 h. Then, 450 μL of HCl (1.2 M) was added and incubated for 1 h. The fluorescence intensity was measured at excitation wavelengths of 312 nm. Fresh HSA solution was used as a control.

Binding of Congo red to amyloid structures can be detected by measuring absorbance at 530 nm.[3] Fluorescence of protein concentration (0.2 mg/mL) in the presence of 10 μM ThT reagent was measured at excitation/emission wavelength of 450/490 nm for determination of the fibrillar state of the protein. This preparation was also used for analysis of aggregation by fluorescence microscopy.[22] The detection of a bright fluorescence against a dim background was considered a positive result for the presence of amyloid. Each time point of these experiments represents the mean of three independent measurements.

Transmission electron micrographs were recorded on a ZEISS electron microscope (EM 902 A) operating at 80 kV. The samples were stained using methylcellulose and uranyl acetate in water. The samples of Rib–HSA precipitates were fixed, dehydrated with ethanol, and embedded in Araldite resin. Thin sections were stained with methylcellulose containing uranyl acetate.

Surface tension was measured at 25 °C with a Krüss K100 tensiometer using the Wilhelmy plate method. The surface tension (γ) of the liquid is related to the force (F) on the plate according to Eq. 4:

$$\gamma = \frac{F}{L\cos\theta} \tag{4}$$

where L is the wetted length and θ is the contact angle. For clean plate surfaces $\theta \approx 0$.

Acknowledgments

The financial support of the Research Council of the University of Tehran and the Iran National Science Foundation (INSF) are gratefully acknowledged. N.S. is a recipient of a research award from American Diabetes Association.

References

1. Lapolla, A.; Traldi, P.; Fedele, D. *Clin. Biochem.* **2005**, *38*, 103–115.
2. Schmitt, A.; Schmitt, J.; Münch, G.; Gasic-Milencovic, J. *Anal. Biochem.* **2005**, *338*, 201–215.
3. Bouma, B.; Kroon-Batenburg, L. M. J.; Wu, Y. P.; Brunjes, B.; Posthuma, G.; Kranenburg, O.; de Groot, P. G.; Voest, E. E.; Gebbink, M. F. B. G. *J. Biol. Chem.* **2003**, *278*, 41810–41819.
4. Chevalier, F.; Chobert, J. M.; Genot, C.; Haertle, T. *J. Agric. Food Chem.* **2001**, *49*, 5031–5038.
5. Chevalier, F.; Chobert, J. M.; Dalgalarrondo, M.; Choiset, Y.; Haertle, T. *Nahr.-Food* **2002**, *46*, 58–63.
6. Trueb, B.; Holenstein, C. G.; Fischer, R. W.; Winterhalter, K. H. *J. Biol. Chem.* **1980**, *255*, 6717–6720.
7. Iberg, N.; Fluckiger, R. *J. Biol. Chem.* **1986**, *261*, 13542–13545.
8. He, X. M.; Carter, D. C. *Nature* **1992**, *358*, 209–215.
9. Coussons, P. J.; Jacoby, J.; McKay, A.; Kelly, S. M.; Price, N. C.; Hunt, J. V. *Free Radical Biol. Med.* **1997**, *22*, 1217–1227.
10. Sharma, S. D.; Pandey, B. N.; Mishra, K. P.; Sivakami, S. *J. Biochem. Mol. Biol. Biophys.* **2002**, *6*, 233–242.
11. Mendez, D. M.; Jensen, R. A.; McElroy, L. A.; Pena, J. M.; Esquerra, R. M. *Arch. Biochem. Biophys.* **2005**, *444*, 92–99.
12. Zoellner, H.; Hou, Y. H.; Hochgrebe, T.; Poljak, A.; Duncan, M. W.; Golding, J.; Henderson, T.; Lynch, G. *Biochem. Biophys. Res. Commun.* **2001**, *284*, 83–89.
13. Voziyan, P. A.; Khalifah, R. G.; Thibaudeau, C.; Yildiz, A.; Jacob, J.; Serianni, A. S.; Hudson, B. G. *J. Biol. Chem.* **2003**, *278*, 46616–46624.
14. Westwood, M. E.; Thornalley, P. J. *J. Protein Chem.* **1995**, *4*, 359–372.
15. Biemel, K. M.; Friedl, D. A.; Lederer, M. O. *J. Biol. Chem.* **2002**, *277*, 24907–24915.
16. Bunn, H. F.; Higgins, P. L. *Science* **1981**, *213*, 222–224.
17. Munanairi, A.; O'Banion, S. K.; Gamble, R.; Breuer, E.; Harris, A. W.; Sandwick, R. K. *Carbohydr. Res.* **2007**, *342*, 2575–2592.
18. Valencia, J. V.; Weldon, S. C.; Quinn, D.; Kirs, G. H.; Degroot, J.; Tekoppele, J. M.; Hughes, T. E. *Anal. Biochem.* **2004**, *324*, 68–78.
19. Barzegar, A.; Moosavi-Movahedi, A. A.; Sattarahmady, N.; Hosseinpour-Faizi, M. A.; Aminbakhsh, M.; Ahmad, F.; Saboury, A. A.; Ganjali, M. R.; Norouzi, P. *Protein Pept. Lett.* **2007**, *14*, 13–18.
20. Sattarahmady, N.; Moosavi-Movahedi, A. A.; Ahmad, F.; Hakimelahi, G. H.; Habibi-Rezaei, M.; Saboury, A. A.; Sheibani, N. *Biochim. Biophys. Acta* **2007**, *1770*, 933–942.
21. Sattarahmady, N.; Khodagholi, F.; Moosavi-Movahedi, A. A.; Heli, H.; Hakimelahi, G. H. *Int. J. Biol. Macromol.* **2007**, *41*, 180–184.
22. Khurana, R.; Coleman, C.; Ionescu-Zanetti, C.; Carter, S. A.; Krishna, V.; Grover, R. K.; Roy, R.; Singh, S. *J. Struct. Biol.* **2005**, *151*, 229–238.
23. Lin, T. Y.; Timasheff, S. N. *Protein Sci.* **1996**, *5*, 372–381.
24. Santos, S. F.; Zanette, D.; Fischer, H.; Itri, R. *J. Colloid Interface Sci.* **2003**, *262*, 400–408.
25. Guzeya, D.; McClements, D. J.; Weissa, J. *Food Res. Int.* **2003**, *36*, 649–660.
26. Makievski, A. V.; Fainerman, V. B.; Bree, M.; Wustneck, R.; Kragel, J.; Miller, R. *J. Phys. Chem. B* **1998**, *102*, 417–425.
27. Messina, P.; Prieto, G.; Dodero, V.; Cabrerizo-Vilchez, M. A.; Maldonado-Valderrama, J.; Ruso, J. M.; Sarmiento, F. *Biopolymers* **2006**, *82*, 261–271.
28. Tofani, L.; Feis, A.; Snoke, R. E.; Berti, D.; Baglioni, P.; Smulevich, G. *Biophys. J.* **2004**, *87*, 1186–1195.
29. Moosavi-Movahedi, A. A. *J. Iran. Chem. Soc.* **2005**, *2*, 189–196.